

Nonparametric Bayes dynamic modeling of relational data

Daniele Durante

*Department of Statistical Sciences
University of Padua
Padua, Italy*

DURANTE@STAT.UNIPD.IT

David B. Dunson

*Department of Statistical Science
Duke University
Durham, NC 27708-0251, USA*

DUNSON@DUKE.EDU

Editor:

Abstract

1 Symmetric binary matrices representing relations among entities are commonly collected
 2 in many areas. Our focus is on dynamically evolving binary relational matrices, with
 3 interest being in inference on the relationship structure and prediction. We propose a
 4 nonparametric Bayesian dynamic model, which reduces dimensionality in characterizing
 5 the binary matrix through a lower-dimensional latent space representation, with the latent
 6 coordinates evolving in continuous time via Gaussian processes. By using a logistic mapping
 7 function from the probability matrix space to the latent relational space, we obtain a flexible
 8 and computational tractable formulation. Employing Pólya-Gamma data augmentation,
 9 an efficient Gibbs sampler is developed for posterior computation, with the dimension of
 10 the latent space automatically inferred. We provide some theoretical results on flexibility
 11 of the model, and illustrate performance via simulation experiments. We also consider an
 12 application to co-movements in world financial markets.

13 **Keywords:** Gaussian process; factor model; latent space; matrix factorization; nonpara-
 14 metric Bayes; co-movement data; financial network.

15 1. Introduction

16 Relational data often take the form of a symmetric binary matrix, with entries indicating the
 17 presence or absence of links between pairs of individuals or entities. In dynamic settings, the
 18 links and the set of entities under consideration can change over time, and interest focuses
 19 on inferences on the time varying relational structure and in prediction. Examples include
 20 social network analysis, in which links encode friendship networks among individuals, and
 21 broader relational settings in which closeness between a pair of units (products, stimuli,
 22 countries, companies, etc) is expressed on a binary scale. Figure 1 shows an example
 23 of time-varying binary similarity matrices encoding dynamic co-movements in National
 24 Stock Market Indices from 2004 to 2013. Co-movements among a set of assets or market
 25 indices are typically analyzed via time-varying covariance or correlation matrices of their
 26 corresponding log-returns $Z_t = [z_{1,t}, z_{2,t}, \dots, z_{V,t}]'$, $t = 1, \dots, T$, (see e.g. Tsay, 2005, Wilson
 27 & Ghahramani, 2010, Nakajima & West, 2012, Durante et al., 2013); we instead provide
 28 a different and not yet fully explored direction of research by treating co-movements as

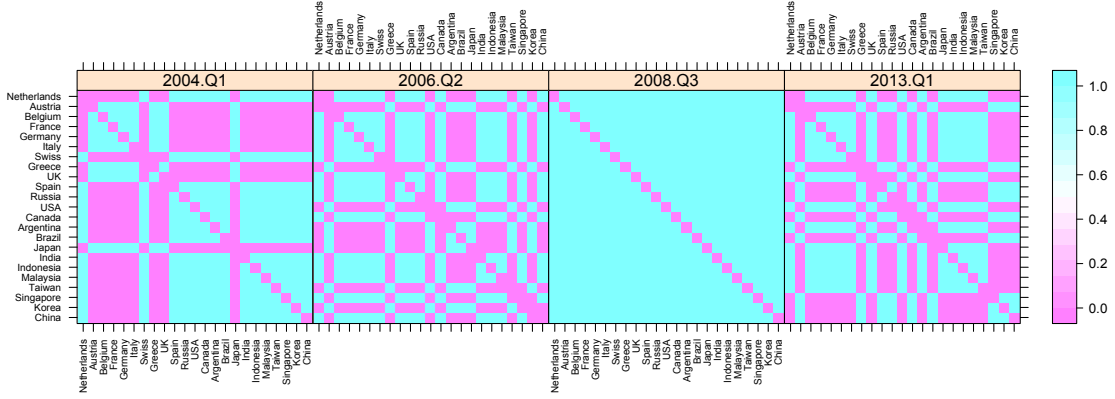


Figure 1: Dynamic co-movements in world financial markets.

dynamic relational data, shifting our attention from Z_t to the $V \times V$ time-varying symmetric matrices $\{Y_t, t \in \mathcal{T} \subset \Re^+\}$. The matrix Y_t has entries $y_{ij,t} = y_{ji,t} = 1$ if index i and index j move in the same direction at time t (i.e. $z_{i,t} > 0$ and $z_{j,t} > 0$, or $z_{i,t} < 0$ and $z_{j,t} < 0$) and $y_{ij,t} = y_{ji,t} = 0$ if they move in opposite directions (i.e. $z_{i,t} > 0$ and $z_{j,t} < 0$, or $z_{i,t} < 0$ and $z_{j,t} > 0$). Co-movements indicate similarity in the indices.

A rich literature is available on modeling similarity or dissimilarity matrices, with Multidimensional Scaling (MDS) providing a widely used technique for graphically representing units in a Euclidean space conditionally on their pairwise dissimilarity measures. General theory and applications are available for Euclidean distances and rank dissimilarities (see Cox & Cox, 2001), with subsequent developments in a Bayesian framework (Oh & Raftery, 2001, Oh & Raftery, 2007) improving the overall performance, but subject to possible issues due to non-identifiable latent coordinates, lack of full conditional conjugacy and absence of an automatic procedure for learning the dimension of the latent space. Moreover, generalizations in the dynamic case are lacking, with only few recent proposals restricted to specific applications for discrete time evolution (Jamali-Rad & Leus, 2012).

When binary similarity or dissimilarity matrices are analyzed, the previous procedures prove to be inappropriate or impractical (Holbrook et al., 1982), with predicted values outside the probability range and a large number of tied ranks for each unit in non-metric MDS applications. Spatial analysis of choice data (DeSarbo & Hoffman, 1987, DeSarbo et al., 1999) provides a possible generalization of MDS for binary variables, with recently developed algorithms available also in the dynamic case (Sarkar et al., 2007). However, questionable independence assumptions are required to ease maximum likelihood estimation, and Bayesian extensions (DeSarbo et al., 1999) to overcome this problem lack scalability in selecting the dimensionality of the latent space via cross-validation methods. Moreover, dynamic extensions via the Kalman filter rely on first and second order Taylor expansions for the observation model, providing difficulties in the derivation of theoretical properties for the exact formulation and requiring a sufficient number of observations to meet the Gaussian assumption. These models are specifically tailored for embedding problems in 2-mode

57 co-occurrence data recording links between two different types of entities (i.e. consumer-
 58 products, author-words). Our focus is instead on dynamic modeling for one-mode binary
 59 matrices.

60 There is a growing body of literature in social networks on model-based statistical
 61 analysis of one-mode binary matrices, traditionally focusing on overly-restrictive models,
 62 such as Erdős & Rényi (1959), the p_1 model (Holland & Leinhardt, 1981) and the Exponential
 63 Random Graph Model (ERGM) (Frank & Strauss, 1986), with generalizations for dynamic
 64 inference available via discrete temporal ERGM (Robins & Pattinson, 2001) and hidden
 65 temporal ERGM (Guo et al., 2007). ERGMs have had growing popularity, but have a
 66 number of drawbacks. Estimation relies on pseudo-likelihood (Strauss & Ikeda, 1990) and
 67 approximate MCMC methods (Snijders, 2002), due to the computational intractability in
 68 a fully likelihood approach. Solutions can be degenerate or nearly-degenerate (Handcock et
 69 al., 2003), and questions remain about coherence, inflexibility and other key issues.

70 An alternative class of models focus on clustering the nodes, based on the pattern of
 71 inter-connections in the network. Stochastic Block Models (SBM) (Nowicki & Snijders,
 72 2001) provide a common framework, with the Infinite Relational Model (IRM) (Kemp et
 73 al., 2006) allowing an unknown number of clusters via a Dirichlet process. Dynamic SBMs
 74 have been recently considered (Ishiguro et al., 2010, Yang et al., 2011, Xu & Hero, 2013).
 75 Ishiguro et al. (2010) focus on discrete dynamic evolution via a hidden Markov model.
 76 Xu & Hero (2013) accommodate continuous time analysis via a state space formulation,
 77 but require sufficient numbers of observations in each block to meet Gaussian assumptions
 78 for the sample mean. They use the extended Kalman filter to linearize the observation
 79 equation, leading to questions of accuracy.

80 We dynamically model binary relational matrices by embedding the nodes in a low-
 81 dimensional latent Euclidean space, with coordinates evolving in continuous time via Gaus-
 82 sian processes and edge probabilities constructed utilizing a logistic mapping function from
 83 the probability matrix space to the dot product of the latent coordinates. Hence, we are
 84 most closely related to the literature on latent space models (Hoff et al., 2002) and Mixed
 85 Membership Stochastic Block models (MMSB) (Airoldi et al., 2008), which allow each node
 86 to belong to multiple blocks with fractional membership. Dynamic latent space models
 87 (Sarkar & Moore, 2005) and MMSB models (Xing et al., 2010) incorporate Gaussian per-
 88 turbations in discrete time and state space models, respectively. Posterior computation
 89 relies on several layers of approximation without theory available to justify accuracy. In
 90 contrast, we provide a simple Gibbs sampling algorithm for our model, which converges to
 91 the exact posterior and infers the dimension of the latent space automatically.

92 The paper is organized as follows. In Section 2, we describe the general model structure
 93 with particular attention to prior specification and theoretical properties. Section 3 provides
 94 the Gibbs sampling steps. A simulation study is examined in Section 4, and an application
 95 to quarterly co-movements in world financial markets is presented in Section 5.

96 2. Dynamic Latent Space Model

97 2.1 Notation and Motivation

98 Let Y_t be the symmetric binary similarity matrix at time $t \in \mathcal{T}$ and $\pi(t)$ be the corresponding
 99 symmetric probability matrix having entries $\pi_{ij}(t) = \pi_{ji}(t) = \text{pr}(y_{ij,t} = 1)$ for every $i =$

¹⁰⁰ $1, \dots, V$ and $j = 1, \dots, V$. Letting

$$y_{ij,t} | \pi_{ij}(t) \sim \text{Bern}(\pi_{ij}(t)), \quad (1)$$

¹⁰¹ independently for each $i = 2, \dots, V$ and $j = 1, \dots, i - 1$, our aim is to define a prior Π_π
¹⁰² for the collection of time-varying probability matrices $\pi_{\mathcal{T}} = \{\pi(t), t \in \mathcal{T}\}$ with the goals
¹⁰³ being to (i) obtain a provably flexible specification, (ii) maintain simple computations,
¹⁰⁴ (iii) perform dimensionality reduction in order to scale to moderately large V settings,
¹⁰⁵ (iv) allow unequal spacing and missing observations and (v) allow predictions including a
¹⁰⁶ measure of predictive uncertainty. Since the matrices are symmetric and the similarities
¹⁰⁷ or dissimilarities of a unit with itself are meaningless, we will focus on modeling the lower
¹⁰⁸ triangular part without taking into account the diagonal elements.

¹⁰⁹ 2.2 Latent space dynamic model formulation

¹¹⁰ We construct $\pi_{ij}(t)$ via a monotonic increasing link function $g(\cdot) : \mathbb{R} \rightarrow [0, 1]$ mapping a
¹¹¹ latent similarity measure among units i and j at time t , $s_{ij}(t) \in \mathbb{R}$, into the probability
¹¹² space. Specifically, we choose $g(\cdot)$ to be the distribution function of the logistic random
¹¹³ variable, obtaining

$$\mathbb{E}[y_{ij,t} | \pi_{ij}(t)] = \pi_{ij}(t) = \frac{1}{1 + e^{-s_{ij}(t)}}, \quad (2)$$

¹¹⁴ for $i = 2, \dots, V$, $j = 1, \dots, i - 1$, and $t \in \mathcal{T}$. Without further assumptions on $s_{ij}(t)$,
¹¹⁵ one needs to model separately $\frac{1}{2}V(V - 1)$ stochastic processes, one for each time-varying
¹¹⁶ similarity measure $s_{ij}(t)$, with $i = 2, \dots, V$, $j = 1, \dots, i - 1$ and $t \in \mathcal{T}$, leading to burdensome
¹¹⁷ computations as V increases and failing to borrow information exploiting the underlying
¹¹⁸ process inducing similarities among the units. In order to reduce the dimensionality of the
¹¹⁹ problem and to learn also the network structure among the units for every t , we express
¹²⁰ the similarity measures $s_{ij}(t)$ as a quadratic combination of a set of latent coordinates for
¹²¹ unit i and unit j . Specifically

$$s_{ij}(t) = \mu(t) + x_i(t)'x_j(t), \quad (3)$$

¹²² where $x_i(t) = [x_{i1}(t), \dots, x_{iH}(t)]'$ for $i = 2, \dots, V$ and $x_j(t) = [x_{j1}(t), \dots, x_{jH}(t)]'$ for
¹²³ $j = 1, \dots, i - 1$, are the vectors of latent coordinates of unit i and j respectively, giving
¹²⁴ rise, together with the baseline $\mu(t)$, to the similarity measure between the two units via a
¹²⁵ projection approach. According to this specification, units with latent coordinates in the
¹²⁶ same directions will have a higher probability of being similar (i.e. $y_{ij,t} = 1$), while units
¹²⁷ with opposite coordinates are more likely to be dissimilar (i.e. $y_{ij,t} = 0$).

¹²⁸ This formulation is also intuitive in practical applications. Recall our motivating ex-
¹²⁹ ample of finance, and assume for simplicity $\mu(t) = 0$ and only two latent coordinates rep-
¹³⁰ resenting for example unexpected inflation and industrial production, respectively. Then
¹³¹ indices of countries with features in the same directions will have a higher probability of
¹³² co-moving, while countries with opposite unexpected inflation and industrial production
¹³³ will more likely move on different directions.

¹³⁴ In matrix notation, equation (3) can be rewritten as

$$S(t) = \mu(t)1_V 1_V' + X(t)X(t)', \quad (4)$$

135 where $S(t)$ is a $V \times V$ real symmetric matrix with latent similarity entries $s_{ij}(t)$ and $X(t) =$
 136 $[x_1(t), x_2(t), \dots, x_V(t)]'$. Note that, assuming without loss of generality $\mu(t) = 0$, the above
 137 decomposition is not unique. For example if we define $X(t)^* = X(t)Q$ with Q a $H \times H$
 138 orthogonal matrix, then $X(t)^*X(t)^* = X(t)QQ'X(t)' = X(t)X(t)'$. If one is interested
 139 also in making inference on the latent coordinates matrix $X(t)$, different proposals are
 140 available in latent factor modeling to ensure identifiability via restrictions (see e.g. Bollen,
 141 1989) or Procrustean transformations (Hoff et al., 2002). However since our focus is on
 142 making inference and prediction on the probability matrices, we follow Ghosh & Dunson
 143 (2009) in avoiding identifiability constraints, as such constraints are not necessary to ensure
 144 identifiability of the induced similarity matrix $S(t)$.

145 It is important to characterize the class of $\pi(t)$ matrices whose lower triangular elements
 146 can be represented as in (2) with latent similarities decomposed as in (4). Theorem 1 and the
 147 corresponding Corollary 2 state that for H sufficiently large, the lower triangular matrix
 148 elements of any symmetric probability matrix have such a representation. For $H \geq V$,
 149 \mathcal{X}_X denotes the space of all $V \times H$ dimensional matrices of arbitrary coordinate functions
 150 mapping from $\mathcal{X} \rightarrow \Re$ and \mathcal{X}_μ the space of all baseline mean functions.

Theorem 1 *Given a symmetric real matrix $S(t)$, $\forall t \in \mathcal{T}$, there exist $\{X(t), \mu(t)\} \in$
 $\mathcal{X}_X \otimes \mathcal{X}_\mu$ such that*

$$S(t) = \mu(t) \times 1_V 1_V' + X(t)X(t)', \quad \forall t \in \mathcal{T}$$

151

Proof. Assume without loss of generality that $\mu(t) = 0$ and take $H \geq V$. Consider

$$X(t) = [P(t) \Lambda(t)^{1/2} \quad 0_{V \times (H-V)}],$$

152 where $P(t)$ is the matrix of the eigenvectors of $S(t)$ and $\Lambda(t)$ the diagonal matrix with the
 153 corresponding eigenvalues. Then $S(t) = P(t)\Lambda(t)P(t)' = X(t)X(t)'$, for every $t \in \mathcal{T}$.

Corollary 2 *Given a symmetric probability matrix $\pi(t)$, $\forall t \in \mathcal{T}$, there exist $\{X(t), \mu(t)\} \in$
 $\mathcal{X}_X \otimes \mathcal{X}_\mu$ such that*

$$\pi_{ij}(t) = \frac{1}{1 + e^{-\mu(t) - \sum_{h=1}^H x_{ih}(t)x_{jh}(t)}}, \quad \forall t \in \mathcal{T}, i = 2, \dots, V, j = 1, \dots, i-1$$

154

155 **Proof.** The proof follows immediately from Theorem 1 and from the fact that the mapping
 156 from $s_{ij}(t)$ to $\pi_{ij}(t)$ is a one-to-one continuous increasing function.

157 This ensures that our specification is sufficiently flexible to characterize any true gen-
 158 erating process, and hence can be viewed as nonparametric given sufficiently flexible priors
 159 for the components.

160 2.3 Prior Specification

161 We aim to specify independent prior distributions Π_X and Π_μ for $X_{\mathcal{T}} = \{X(t), t \in \mathcal{T}\}$ and
 162 $\mu_{\mathcal{T}} = \{\mu(t), t \in \mathcal{T}\}$ in order to induce a prior Π_π for $\pi_{\mathcal{T}} = \{\pi(t), t \in \mathcal{T}\}$ through (2) and (3).
 163 This prior is carefully defined to have large support, favor simple and efficient computation,

allow missing values, induce a continuous time specification, and allow learning of the latent space dimension. Bhattacharya & Dunson (2011) proposed a useful approach for Bayesian learning of the number of latent factors in a model for a single large covariance matrix, and we extend their approach from independent Gaussian latent factors to Gaussian process latent factors. In particular, we let

$$x_{ih}(\cdot) \sim \text{GP}(0, \tau_h^{-1} c_X),$$

independently for all $i = 1, \dots, V$ and $h = 1, \dots, H$, with c_X a squared exponential correlation function $c_X(t, t') = \exp(-\kappa_X \|t - t'\|_2^2)$, which allows for continuous time analysis and unequal spacing, and τ_h^{-1} a shrinkage parameter defined as

$$\tau_h = \prod_{k=1}^h \vartheta_k, \quad \vartheta_1 \sim \text{Ga}(a_1, 1), \quad \vartheta_k \sim \text{Ga}(a_2, 1), \quad k \geq 2.$$

Note that if $a_2 > 1$ the expected value for ϑ_k is greater than 1. As a result, as h goes to infinity, τ_h tends to infinity, shrinking $x_{ih}(\cdot)$, for every $i = 1, \dots, V$ towards zero. This leads to a flexible prior for $x_{ih}(\cdot)$ with a local shrinkage parameter τ_h^{-1} that favors many stochastic processes of latent coordinates being close to 0 as h increases. To conclude prior specification we choose

$$\mu(\cdot) \sim \text{GP}(0, c_\mu),$$

with $c_\mu(t, t') = \exp(-\kappa_\mu \|t - t'\|_2^2)$.

Before proceeding with posterior computation, we focus on the support of the induced prior Π_π based on priors Π_X and Π_μ . Specifically we are interested in proving whether the prior can generate a time-varying symmetric probability matrix that is arbitrarily close to any function $\{\pi(t), t \in \mathcal{T}\}$. Intuitively, large support on continuous symmetric similarity matrix functions $\{S(t), t \in \mathcal{T}\}$ relies on the continuity of the Gaussian process coordinate functions. Since for each fixed $t = t_0$, $x_{ih}(t_0)$ are independently Gaussian distributed, $X(t_0)X(t_0)'$ is distributed according to a sum of independent Wishart random variables. Combining the large support of the Wishart distribution with the one of the Gaussian for the baseline $\mu(t_0)$, provides large support for the induced prior Π_S . Since $\pi(t)$ is obtained via a one to one continuous increasing function of $S(t)$, we will map non-null probability subsets of the space of $S(t)$ into non-null probability subsets of the space of $\pi(t)$, providing the desired large support for the induced prior Π_π . Theorem 3 states the large support property for Π_S , while Corollary 4 provides the same property for Π_π by combining results in the previous Theorem with the fact that $\pi(t_0)$ is defined as a monotonic increasing continuous function of $S(t_0)$. Proof of Theorem 3 is provided in Appendix.

Theorem 3 *Let Π_S denote the induced prior on $\{S(t), t \in \mathcal{T}\}$ based on the specified prior $\Pi_X \otimes \Pi_\mu$ on $\mathcal{X}_X \otimes \mathcal{X}_\mu$. Assuming \mathcal{T} compact, for all continuous $S^*(t)$ and for all $\epsilon > 0$*

$$\Pi_S \left(\sup_{t \in \mathcal{T}} \|S(t) - S^*(t)\|_2 < \epsilon \right) > 0.$$

193

Corollary 4 Let Π_π denote the induced prior on $\{\pi(t), t \in \mathcal{T}\}$ based on the specified prior $\Pi_X \otimes \Pi_\mu$ on $\mathcal{X}_X \otimes \mathcal{X}_\mu$. Assuming \mathcal{T} compact, for all continuous $\pi^*(t)$ and for all $\delta > 0$

$$\Pi_\pi \left(\sup_{t \in \mathcal{T}} \|\pi(t) - \pi^*(t)\|_2 < \delta \right) > 0.$$

194

Proof. Since the elements of $\pi(t)$ are defined as a one to one continuous mapping of the elements of $S(t)$ through the function $g(\cdot)$, by definition of continuity we have that for every $\delta > 0$ there exists an $\epsilon > 0$ such that

$$\sup_{t \in \mathcal{T}} \|g(S(t)) - g(S^*(t))\|_2 = \sup_{t \in \mathcal{T}} \|\pi(t) - \pi^*(t)\|_2 < \delta$$

195 for all $S(t)$ such that $\sup_{t \in \mathcal{T}} \|S(t) - S^*(t)\|_2 < \epsilon$, where $g(S(t))$ means that the func-
196 tion $g(\cdot)$ is applied to every element of $S(t)$. Finally, since by Theorem 3 the event
197 $\sup_{t \in \mathcal{T}} \|S(t) - S^*(t)\|_2 < \epsilon$ has non-null probability, it follows that the same holds for
198 the event $\sup_{t \in \mathcal{T}} \|\pi(t) - \pi^*(t)\|_2 < \delta$, completing the proof.

199 3. Posterior computation

200 Posterior computation is performed adapting a recently proposed data-augmentation scheme
201 based on a new class of Pólya-Gamma distributions; for a detailed description see Polson
202 et al. (2013). The approach provides a strategy for fully Bayesian inference in models with
203 binomial likelihoods, which bypasses the need for analytic approximations, while allowing
204 us to exploit conjugacy for block updating.

205 The main result is that binomial likelihoods parameterized by log-odds can be repre-
206 sented as a mixture of Gaussians with respect to Pólya-Gamma distributions. Specifically

$$\frac{(e^\psi)^a}{(1 + e^\psi)^b} = 2^{-b} e^{z\psi} \int_0^{+\infty} e^{-\omega\psi^2/2} p(\omega) d\omega,$$

207 where $z = a - b/2$ and $\omega \sim \text{PG}(b, 0)$, with $\text{PG}(b, c)$ denoting the Pólya-Gamma random
208 variable with parameters $c \in \Re$ and $b > 0$. When $\psi = x'\beta$ is a linear predictor, and
209 a Gaussian prior is considered for β , full conditional conjugacy is ensured for Bayesian
210 inference on the coefficients. Moreover the implied conditional distribution for ω , given ψ ,
211 is again Pólya-Gamma, providing a simple Gibbs sampler alternating between two main
212 steps. Specifically, letting y_i be the number of successes and $x_i = [x_{i1}, \dots, x_{ip}]'$ the vector
213 of regressors for every observation $i = 1, \dots, N$, and assuming a Bayesian logistic regression
214 setting where $y_i \sim \text{Bern}(1/[1 + e^{-\psi_i}])$, $\psi_i = x'_i \beta$ and β having Gaussian prior $\beta \sim \text{N}_p(b, B)$,
215 the Gibbs alternates between

$$\omega_i | \beta, x_i \sim \text{PG}(1, x'_i \beta) \quad \text{and} \quad \beta | y, \omega, x \sim \text{N}_p(\mu_\beta, \Sigma_\beta),$$

216 where $\Sigma_\beta = (X' \Omega X + B^{-1})^{-1}$ and $\mu_\beta = \Sigma_\beta (X' z + B^{-1} b)$; with $z = [y_1 - 1/2, \dots, y_N - 1/2]'$
217 and Ω is the diagonal matrix with ω_i 's entries.

218 Recalling model (1), with probabilities defined as in (2) and latent similarities from (3),
219 for $i = 2, \dots, V$, $j = 1, \dots, i-1$ and $t \in \mathcal{T}_0 = \{t_1, \dots, t_T\}$, and taking a fixed truncation level
220 H^* for the number of latent coordinates, the Gibbs sampler for our model, is:

- 221 1. Update each augmented data $\omega_{ij,t}$ from the full conditional Pólya-Gamma posterior:

$$\omega_{ij,t} | x_i(t), x_j(t), \mu(t) \sim \text{PG} \left(1, \mu(t) + \sum_{h=1}^{H^*} x_{ih}(t) x_{jh}(t) \right)$$

222 for every $i = 2, \dots, V, j = 1, \dots, i-1$ and $t \in \mathcal{T}_0 = \{t_1, \dots, t_T\}$.

- 223 2. Given $\{y_{ij,t}\}, X(t)$ and $\{\omega_{ij,t}\}$, the Pólya-Gamma data augmentation scheme ensures
224 full conditional Gaussian posterior for $\mu(t)$ with $t \in \mathcal{T}_0 = \{t_1, \dots, t_T\}$, of the form

$$\begin{bmatrix} \mu(t_1) \\ \mu(t_2) \\ \vdots \\ \mu(t_T) \end{bmatrix} | \{y_{ij,t}\}, X(t), \{\omega_{ij,t}\} \sim N_T \left(\Sigma_\mu \begin{bmatrix} \sum_{i=2}^V \sum_{j=1}^{i-1} (y_{ij,t_1} - 0.5 - \omega_{ij,t_1} x_i(t_1)' x_j(t_1)) \\ \sum_{i=2}^V \sum_{j=1}^{i-1} (y_{ij,t_2} - 0.5 - \omega_{ij,t_2} x_i(t_2)' x_j(t_2)) \\ \vdots \\ \sum_{i=2}^V \sum_{j=1}^{i-1} (y_{ij,t_T} - 0.5 - \omega_{ij,t_T} x_i(t_T)' x_j(t_T)) \end{bmatrix}, \Sigma_\mu \right)$$

225 With $\Sigma_\mu = [\text{diag}(\sum_{i=2}^V \sum_{j=1}^{i-1} \omega_{ij,t_1}, \dots, \sum_{i=2}^V \sum_{j=1}^{i-1} \omega_{ij,t_T}) + K_\mu^{-1}]^{-1}$, and K_μ the
226 Gaussian process covariance matrix with $[K_\mu]_{ij} = \exp(-\kappa_\mu \|t_i - t_j\|_2^2)$.

- 227 3. Update the time-varying latent coordinate vector $\{x_v(t) = [x_{v1}(t), \dots, x_{vH^*}(t)]'\}_{t=t_1}^{t_T}$
228 for every unit $v = 1, \dots, V$ from its conditional posterior. Specifically, conditionally on
229 $X^{(-v)} = \{x_j(t) : j \neq v, t \in \mathcal{T}_0 = \{t_1, \dots, t_T\}\}$, $\mu = [\mu(t_1), \dots, \mu(t_T)]'$, $\{y_{ij,t}\}$, $\{\omega_{ij,t}\}$,
230 $\{\tau_h\}$ and defining $y_{ij} = [y_{ij,t_1}, \dots, y_{ij,t_T}]'$ and $\pi_{ij} = [\pi_{ij,t_1}, \dots, \pi_{ij,t_T}]'$, let $Y^{(v)}$ be the
231 vector obtained by stacking sub-vectors y_{ij} for all the couples (i, j) such that $i = v$ or
232 $j = v$, with $i > j$; and $\pi^{(v)}$ the corresponding vector of probabilities, then

$$\text{logit}(\pi^{(v)}) | X^{(-v)}, \mu(t) = 1_{V-1} \otimes \mu + \tilde{X}_{x_v(t)} \beta_{x_v(t)} \quad (5)$$

where $\beta_{x_v(t)} = [x_{v1}(t_1), \dots, x_{v1}(t_T), x_{v2}(t_1), \dots, x_{v2}(t_T), \dots, x_{vH^*}(t_1), \dots, x_{vH^*}(t_T)]'$ with prior, according to GP formulation, $\beta_{x_v(t)} \sim N_{T \times H^*}(0, \text{diag}[\tau_1^{-1}, \dots, \tau_{H^*}^{-1}] \otimes K_x)$ and $\tilde{X}_{x_v}(t)$ a matrix of regressors with entries suitably chosen from the elements of $X^{(-v)}$ in order to reproduce the equality:

$$\text{logit}(\pi_{ij}(t)) | X(t), \mu(t) = \mu(t) + \sum_{h=1}^{H^*} x_{ih}(t) x_{jh}(t)$$

233 for all the probabilities $\pi_{ij}(t)$ such that $i = v$ or $j = v$, with $i > j$ and $t \in \mathcal{T}_0 = \{t_1, \dots, t_T\}$. Model (5) is a proper logistic regression with linear predictor, therefore,
234 according to our Pólya-Gamma sampling scheme, we update the vector of time-varying
235 coordinates $\{x_v(t) = [x_{v1}(t), \dots, x_{vH^*}(t)]'\}_{t=t_1}^{t_T}$, represented by $\beta_{x_v(t)}$ by sampling from:
236

$$\beta_{x_v(t)} | X^{(-v)}, \{\mu(t)\}, \{y_{ij,t}\}, \{\omega_{ij,t}\}, \{\tau_h\} \sim N_{T \times H^*}(\mu_{x_v(t)}, \Sigma_{x_v(t)})$$

237 with

$$\begin{aligned} \Sigma_{x_v(t)} &= \left(\tilde{X}'_{x_v(t)} \Omega_{x_v(t)} \tilde{X}_{x_v(t)} + \text{diag}[\tau_1, \dots, \tau_{H^*}] \otimes K_x^{-1} \right)^{-1} \\ \mu_{x_v(t)} &= \Sigma_{x_v(t)} \left[\tilde{X}'_{x_v(t)} (Y^{(v)} - 1_{V-1} \otimes 1_T \times 0.5 - 1_{V-1} \otimes \mu) \right] \end{aligned}$$

238 and $\Omega_{x_v(t)}$ is the diagonal matrix with the corresponding Pólya-Gamma augmented
239 data.

240 4. Conditioned on $X(t)$ and $\{\tau_h\}$, sample the global shrinkage hyperparameters from

$$\begin{aligned}\vartheta_1|X(t), \tau^{(-1)} &\sim \text{Ga} \left(a_1 + \frac{V \times T \times H^*}{2}, 1 + \frac{1}{2} \sum_{l=1}^{H^*} \tau_l^{(-1)} \sum_{i=1}^V x'_{il} K_x^{-1} x_{il} \right) \\ \vartheta_h|X(t), \tau^{(-h)} &\sim \text{Ga} \left(a_2 + \frac{V \times T \times (H^* - h + 1)}{2}, 1 + \frac{1}{2} \sum_{l=1}^{H^*} \tau_l^{(-h)} \sum_{i=1}^V x'_{il} K_x^{-1} x_{il} \right)\end{aligned}$$

241 Where $\tau_l^{(-h)} = \prod_{t=1, t \neq h}^l \vartheta_t$ for $h = 1, \dots, H^*$ and $x_{il} = [x_{il}(t_1), \dots, x_{il}(t_T)]'$.

242 We can easily handle missing values by adding a further step imputing the unobserved
 243 binary similarities from their conditional distribution given the current state of the chain.
 244 Specifically:

245 5. Given $X(t)$ and $\mu(t)$ sample each missing value from its conditional distribution

$$y_{ij,t} = y_{ji,t}|X(t), \mu(t) \sim \text{Bern} \left(\frac{1}{1 + e^{-\mu(t) - \sum_{h=1}^{H^*} x_{ih}(t)x_{jh}(t)}} \right), \quad i > j.$$

246 Step 5 provides also a strategy for predicting new outcomes. Specifically, if we are interested
 247 in making inference on future $\pi(t_{T+1})$ with $t_{T+1} > t_T$ given the observed similarity matrices
 248 Y_t , $t \in \mathcal{T}_0 = \{t_1, \dots, t_T\}$, then we can simply perform the previous posterior computations
 249 adding to the observed dataset $\{Y_t\}_{t \in \mathcal{T}_0}$ a new matrix $Y_{t_{T+1}}$ of missing values and make
 250 inference on the predictive posterior distribution using the samples of the Markov chain for
 251 $\pi(t_{T+1})$.

252 4. Simulation Study

253 We provide a simulation study with the aim to evaluate the performance of the proposed
 254 model in analyzing a dataset constructed to mimic also a possible generating process in the
 255 finance application. The focus is on the ability to correctly reconstruct the true underlying
 256 processes, and also on the performance with respect to out of sample predictions. We
 257 also provide a comparison between our proposed approach and the estimated probability
 258 process for each time-varying binary outcome when using only temporal information without
 259 exploring matrix structure, showing graphically the sub-optimality of the latter in terms of
 260 efficiency and bias.

261 4.1 Estimating Performance

262 We generate a set of 15×15 time varying Y_t matrices with t in the discrete set $\mathcal{T}_0 =$
 263 $\{1, 2, \dots, 40\}$. Each $y_{ij,t}$ is simulated according to (1) with probabilities obtained from (2)
 264 and (3), generating $\{\mu(t)\}_{t=1}^{40}$ from a $\text{GP}(0, c_\mu)$ with length scale $\kappa_\mu = 0.01$ and choosing
 265 2 time-varying latent coordinates $\{x_{i1}(t)\}_{t=1}^{40}$, $\{x_{i2}(t)\}_{t=1}^{40}$ from Gaussian processes with
 266 length scale $\kappa_x = 0.01$, independently for each unit $i = 1, \dots, 15$. To evaluate the out of
 267 sample predictive performance we take Y_{40} to be a matrix of missing values, and assume
 268 similarities between units 10 and 11 and all the others, missing at times $t = 20, \dots, 25$ to
 269 assess the behavior with respect to missing data. For inference we choose a truncation level

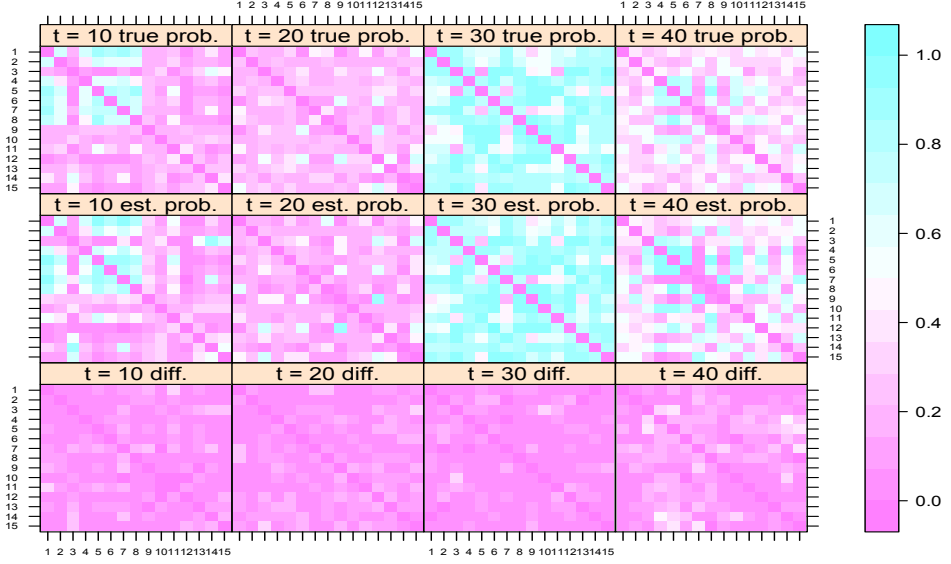


Figure 2: For some selected times t , plot of the true probability matrix $\pi(t)$ (top), posterior mean $\hat{\pi}(t)$ from our model (middle) and absolute value of the difference among the two $|\pi(t) - \hat{\pi}(t)|$ (bottom).

270 $H^* = 10$, length scales $\kappa_\mu = \kappa_x = 0.05$ and set $a_1 = a_2 = 2$ for the shrinkage parameters.
271 We ran 5,000 Gibbs iterations which proved to be enough for reaching convergence and
272 discarded the first 1,000. Mixing was assessed by analyzing the effective sample sizes of the
273 MCMC chains for the quantities of interest (i.e. $\pi_{ij}(t)$, for $i = 2, \dots, V$, $j = 1, \dots, i-1$ and
274 $t \in \mathcal{T}_0$) after burn-in. We found most of these values concentrating around $\approx 1,700$ effective
275 samples on a total of 4,000, providing a good mixing result.

276 The comparison in Figure 2 between true probability matrices and their corresponding
277 posterior mean for some selected time t , highlights the good performance of our approach
278 in correctly estimating the true latent process and making predictions. The latter can be
279 noticed by comparing true and estimated probability matrices at $t = 40$, recalling that in
280 our simulation we assumed Y_{40} having missing entries and we were interested in analyzing
281 the predictive performance of our model with respect to $\pi(40)$. Similar results are provided
282 by the plot of true $\pi_{ij}(t)$ against the corresponding estimates $\hat{\pi}_{ij}(t)$ and by the ROC curve
283 in Figure 3 having an area underneath of 0.87.

284 Figure 4 shows a graphical comparison between the performance of our model with
285 respect to $\mu(t)$ and some selected probability trajectories $\pi_{ij}(t)$ (top), and the inferential
286 results when the mean process and probability process $\pi_{ij}(t)$ are estimated with the same
287 setting of our model but using only the time series of the corresponding $y_{ij,t}$ without bor-
288 rowing information across the network (bottom). The sub-optimality of the independent
289 approach is apparent in terms of both bias (over-smoothed trajectories) and variance (larger

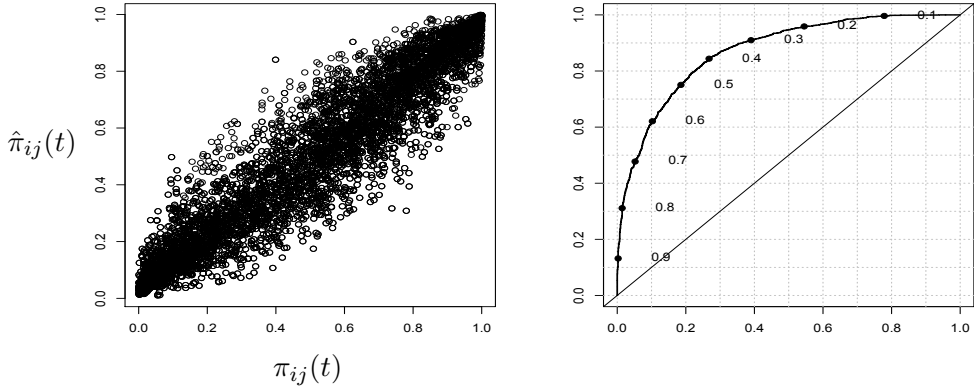


Figure 3: Left: plot of true probabilities $\pi_{ij}(t)$ versus their corresponding posterior mean $\hat{\pi}_{ij}(t)$, for $i = 2, \dots, V$, $j = 1, \dots, i - 1$ and $t \in \mathcal{T}_0$. Right: ROC curve generated using $\hat{\pi}_{ij}(t)$ and the observed data Y_t .

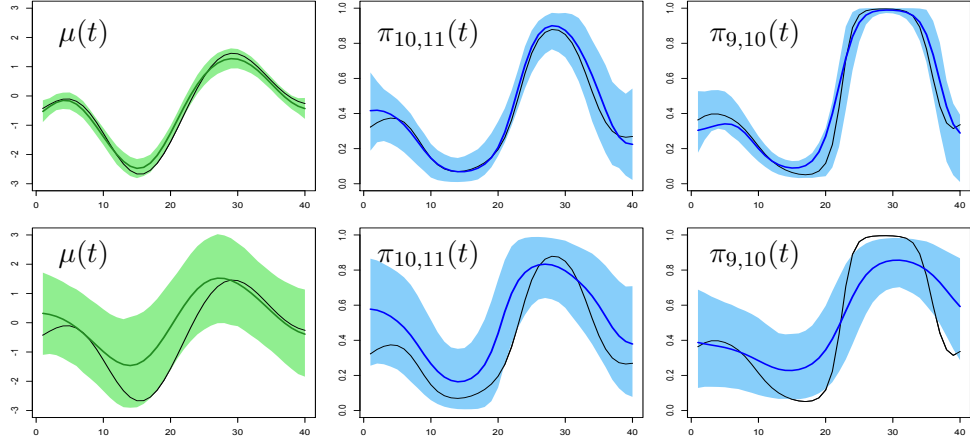


Figure 4: Top: For $\mu(t)$ and some selected $\pi_{ij}(t)$, plot of the true trajectory (black line), point-wise posterior mean (colored lines) and 0.95 highest posterior density (hpd) intervals (colored areas) for our model. Bottom: Same quantities estimated using only temporal information without exploring network structure (i.e. estimate $\pi_{ij}(t)$ using only the time series of the corresponding $y_{ij,t}$)

290 hpd intervals). When network structure is taken into account, the model provides accurate
 291 estimates, with posterior distributions rapidly concentrating around the true corresponding
 292 processes, while accurately selecting the dimension of the latent space. In particular, we
 293 find that the estimated $\hat{\tau}_h^{-1}$ values start at 0.8 and 0.7 for $h = 1$ and 2, respectively, but then
 294 drop to small values for the later factors. This implies that these later factor trajectories
 295 are quite flat and have limited influence. Borrowing information across the network over
 296 time has the additional advantage of reducing hyperparameter sensitivity, in particular with
 297 respect to the length scale in GP prior. We obtain, in fact, similar results when instead
 298 letting $\kappa_\mu = \kappa_x = 0.03$, $\kappa_\mu = \kappa_x = 0.1$ and $\kappa_\mu = \kappa_x = 0.5$ in sensitivity analyses.

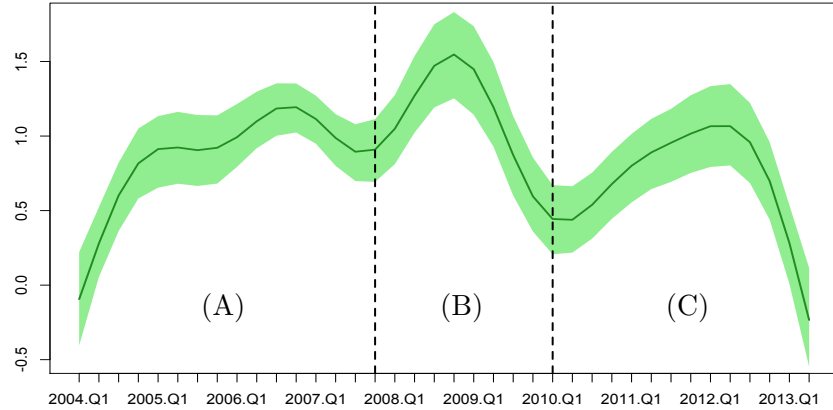


Figure 5: Plot of the point-wise posterior mean for the baseline $\mu(t)$ (colored line), and 0.95 hpd intervals (colored areas). (A) Growth and burst of USA housing bubble, (B) Global financial crisis, (C) Greek debt crisis, worsening of European sovereign-debt crisis and the rejection of the U.S. budget.

299 5. Application to co-movements among National Stock Market Indices

300 National Stock Indices represent technical tools constructed by a synthesis of numerous
 301 data on the evolution of the various stocks, and represent important indicators of the
 302 financial condition in a given country. Modeling co-variations among these quantities, and
 303 in general among assets, represents a fundamental issue in many financial applications,
 304 such as the Arbitrage Pricing Theory (APT) of Ross (1976) and the Capital Asset Pricing
 305 Model (CAPM) developed by Sharpe (1964), and the correlations or covariances among
 306 asset's returns are the typical measures of co-movements employed in this framework.

307 A rich literature is available in modeling dynamic covariance or correlation matrices,
 308 covering multivariate generalizations of ARCH and GARCH models (see e.g. Tsay, 2005,
 309 Engle, 2002, Alexander, 2001, Bollerslev et al., 1988), Stochastic volatility models (Harvey et
 310 al., 1994) and recent Bayesian extensions (see e.g. Wilson & Ghahramani, 2010, Nakajima
 311 & West, 2012, Durante et al., 2013). In this application, we instead provide a different
 312 and not fully explored measure of co-movement exploiting the network structure among
 313 financial indices and giving exactly the probability that such event happens at a given
 314 time. This is accomplished by applying our model to the time-varying Y_t matrices having
 315 entries $y_{ij,t} = y_{ji,t} = 1$ if index i and index j co-move at time t (indices are similar), and
 316 $y_{ij,t} = y_{ji,t} = 0$ if opposite increments are recorded (indices are dissimilar).

317 We constructed Y_t using the quarterly log-returns of the 23 main National Stock Market
 318 Indices ($V = 23$) from 2004 to 2013 ($T = 39$, with the last empty matrix Y_{39} used for prediction),
 319 available at <http://finance.yahoo.com/> and applied model (1), with probabilities
 320 specified as in (2) and latent similarity measures obtained via the projection approach de-
 321 fined in (3). For posterior computation we run 5,000 Gibbs iterations with a burn-in of 1,000,
 322 setting a truncation level $H^* = 15$, length scales $\kappa_\mu = 0.03$, $\kappa_x = 0.01$ and $a_1 = a_2 = 2$.
 323 Similarly to the simulation study, most of the chains have effective sample sizes around

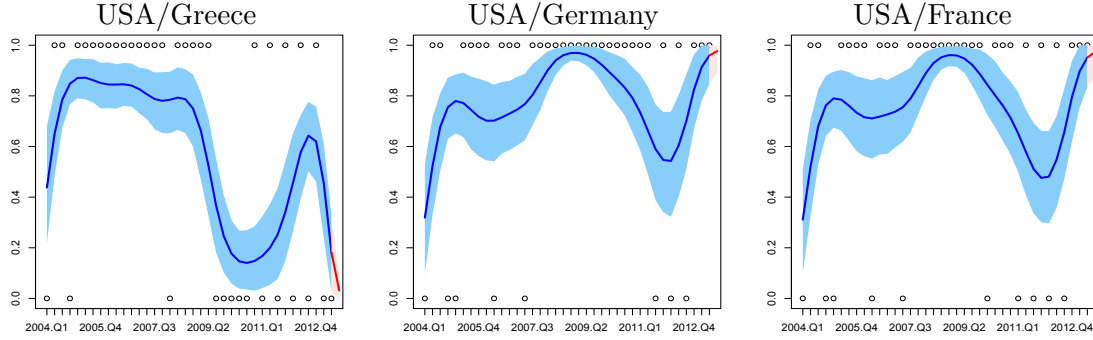


Figure 6: Observed data (black dots), estimated co-movement probability trajectories (blue lines) and 0.95 highest posterior density intervals (colored blue areas), among USA and some selected European countries. Red lines and areas represent the same quantities with respect to posterior predictive distribution.

324 1,600 on a total of 4,000 after burn-in, showing good mixing. We find that the first two
 325 latent factors are the most informative, with the remaining 13 latent processes being con-
 326 centrated near zero. A similar result was obtained in the seminal work of Fama & French
 327 (1993), providing three main common risk factors in the returns of stocks.

328 5.1 Model Interpretation

329 The estimated trajectory of the baseline process $\mu(t)$ together with the point-wise 0.95 hpd
 330 intervals in Figure 5, provide important insights on the overall financial market behavior,
 331 in agreement with other theories on financial crises (see, e.g., Baig and Goldfajn, 1999,
 332 and Claessens & Forbes, 2009) and recent applications (Durante et al., 2013, Kastner et al.,
 333 2013). Increasing and persistent level of the baseline process, inducing higher probability of
 334 co-movements, are recorded during the growth and burst of USA housing bubble and the
 335 initial turmoils before the 2008 global financial crisis (A). This result provides an empirical
 336 proof in favor of the increasing inter-connection among financial markets due to the prolif-
 337 eration of risky loans between 2004 and 2007, and the growing demand by foreign countries
 338 for financial assets built from the real estate market, such as residential mortgage-backed
 339 securities (RMBS) and collateralized debt obligations (CDO). As expected the global finan-
 340 cial crisis between late-2008 and end-2009 (B), and the following, Greek debt crisis together
 341 with the worsening of European sovereign-debt crisis (C), are manifested through a further
 342 increase of the co-movement probabilities, highlighting a clear financial contagion effect.

343 Figure 6 shows the estimated (blue lines) and predicted (red lines) co-movement prob-
 344 ability trajectories among USA and some selected European countries, pointing out the
 345 good performance of the proposed model in adaptively learning the data structure, con-
 346 firmed also by a ROC curve having an area underneath of 0.79. It is worth noticing that
 347 the local adaptivity of the estimated trajectories is not due to an over-parameterization of
 348 the model since the shrinkage prior on τ_h and the choice of small length scales in the GP co-
 349 variance functions, imply smooth trajectories and a parsimonious model formulation. Thus
 350 adaptivity is provided by the information borrowed in the financial network for each time t .
 351 Co-movement probabilities among USA and Greece register a sharp drop in correspondence
 352 of the Greek debt crisis, differently from what happens with other European countries such

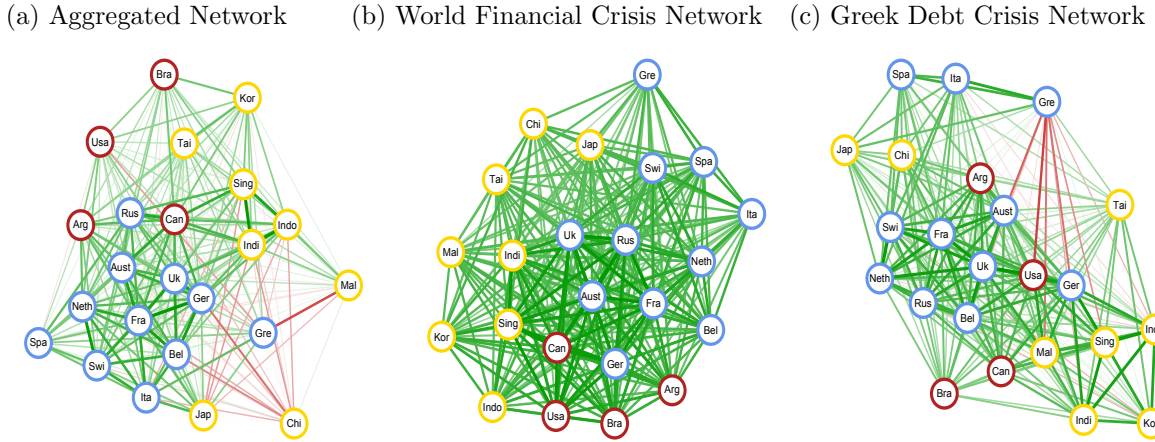


Figure 7: Left: weighted network visualization with weights obtained averaging $\hat{\pi}(t)$ over T_0 . Middle: weighted network visualization with weights obtained averaging $\hat{\pi}(t)$ over the period of Global Financial Crisis (end 2008, beginning 2009). Right: Middle: weighted network visualization with weights obtained averaging $\hat{\pi}(t)$ over the period of Greek debts Crisis. Edge dimensions are proportional to the corresponding value of the averaged probability matrix, with colors going from red to green gradation as the corresponding weight goes from 0 to 1. Blue, Red and Yellow nodes represent European, American and Asian countries, respectively.

as Germany and France, which instead evolve on similar patterns. We found this result reasonable in providing an empirical proof on the attempt to reduce the inter-connection with a country in crisis.

Finally, Figure 7 provides interesting insights on the financial network structure among the countries under investigation. Specifically we represent three different weighted networks, with weights given by the average estimated co-movement probability over all the time window considered (a), the estimated probability averaged over the period of the global financial crisis (b), and the Greek debt crisis (c). A reasonable global network structure with countries having similar financial economies most closely related among each other is provided in plot (a). As expected Japan appears to be closer to Western economies than Asian financial markets, while China has lower inter-connections with other countries. Stronger networks are estimated for European markets and Asian Tigers. International financial contagion effect is highlighted through strong inter-connections among all financial markets during the 2008 global financial crisis (b), with a still evident clustering effect, and Greece already showing a slightly different behavior. Finally, when the network during the Greek debt crisis is analyzed, we register evident low connections among Greece and almost all the other financial markets considered, and interestingly learn a strong network between Greece, Spain and Italy, representing the countries most affected by the European sovereign-debt crisis.

6. Discussion

We proposed a Bayesian nonparametric dynamic model for binary similarity matrices, borrowing information across time and the network structure of the data under investigation

and allowing for dimensionality reduction. The model has been constructed using latent similarity measures defined by the dot product of latent coordinate vectors, with entries evolving in continuous time via Gaussian process priors. The shrinkage hyperprior allows us to automatically learn the dimension of the latent space and ensures a parsimonious definition of the model, with the risk of over-parameterization due to a higher number of latent features avoided. The Pólya-Gamma data augmentation strategy allows us to define a simple and efficient Gibbs sampler for posterior computations based on full conditional conjugate posterior distributions, which is promising in terms of scaling to moderately large V , and easily handling missing values as well as forecasting problems. Scalability to large T could be, instead, improved via stochastic differential equations models approximating the GP prior on the latent coordinate processes (Zhu and Dunson, 2012). We provided also theoretical results on the flexibility of the model, illustrated its performance via a simulation study and obtained interesting insights on the network among financial markets during the recent crisis, by applying the model to time-varying co-movement data.

Our model has a broad range of applicability, with dynamic social network analysis and time-varying binary evaluations among units providing two natural fields of application. Further directions of research could be devoted to the definition of similar models for discrete valued dynamic matrices, which could provide useful tools for analyzing edge valued dynamic social networks or datasets with comparison among units expressed on a Likert scale.

References

- Airoldi, E.M., Blei, D.M., Fienberg, S.E., & Xing, E.P. (2008). Mixed Membership Stochastic Blockmodels. *Journal of Machine Learning Research* 9, 1981–2014.
- Alexander, C.O. (2001). Orthogonal GARCH. *Mastering Risk* 2, 21–38.
- Baig, T., & Goldfajn, I. (1999). Financial Market Contagion in the Asian Crisis. *Staff Papers, International Monetary Fund* 46, 167–195.
- Bhattacharya, A., & Dunson, D.B. (2011). Sparse Bayesian infinite factor models. *Biometrika* 98, 291–306.
- Bollen, K.A. (1989). *Structural Equations with Latent Variables*. Wiley.
- Bollerslev, T., Engle, R.F., & Wooldridge, J.M. (1988). A capital-asset pricing model with time-varying covariances. *Journal of Political Economy* 96, 116–131.
- Claessens, S., & Forbes, K. (2009) International Financial Contagion, An overview of the Issues. Springer.
- Cox, T.F., & Cox, M.A. (2001). *Multidimensional Scaling*. II ed., Chapman and Hall.
- DeSarbo, W.S., Kim, Y., & Fong D. (1999). A Bayesian multidimensional scaling procedure for the spatial analysis of revealed choice data. *Journal of Econometrics* 89, 79–108.

- 411 DeSarbo, W.S., & Hoffman, D.L. (1987). Constructing MDS joint spaces from binary choice
412 data: A new multidimensional unfolding threshold model for marketing research. *Journal*
413 *of Marketing Research* 24, 40–54.
- 414 Durante, D., Scarpa, B. & Dunson, D.B. (2013). Locally adaptive factor processes for
415 multivariate time series. <http://arxiv.org/abs/1210.2022>.
- 416 Engle, R.F. (2002). Dynamic conditional correlation: a simple class of multivariate gener-
417 alized autoregressive conditional heteroskedasticity models. *Journal of Business & Eco-*
418 *nomic Statistics* 20, 339–350.
- 419 Erdős, P., & Rényi, A. (1959). On Random Graphs *Publicationes Mathematicae* 6, 290–297.
- 420 Fama, E.F., & French, K.R. (1993). Common risk factors in the returns on stocks and
421 bonds. *Journal of Financial Economics* 33, 3–56.
- 422 Frank, O., & Strauss, D. (1986). Markov Graphs. *Journal of the American Statistical*
423 *Association* 81, 832–842.
- 424 Ghosh, J., & Dunson, D.B. (2009) Default priors and efficient posterior computation in
425 Bayesian factor analysis. *Journal of Computational and Graphical Statistics* 18, 306–
426 320.
- 427 Guo, F., Hanneke S., Fu, W., & Xing, E.P. (2007). Recovering temporally rewiring networks:
428 A model-based approach. In *International Conference in Machine Learning*.
- 429 Handcock, M.S., Robins, G.L., Snijders, T.A.B., Moody, J., & Besag, J. (2003). Assessing
430 Degeneracy in Statistical Models of Social Networks. *Journal of the American Statistical*
431 *Association* 76, 33–50.
- 432 Harvey, A.C., Ruiz E., & Shepard N. (1994). Multivariate stochastic variance models.
433 *Review of Economic Studies*, 61, 247–264.
- 434 Hoff, P.D., Raftery, A.E., & Handcock, M.S. (2002). Latent Space Approaches to Social
435 Network Analysis. *Journal of the American Statistical Association* 97, 1090–1098.
- 436 Holbrook M.B., William L.M., & Russell S.W. (1982). Constructing Joint Spaces from
437 “Pick-Any” Data: A New Tool for Consumer Analysis. *Journal of Consumer Research* 9,
438 99–105.
- 439 Holland, P.W., & Leinhardt, S. (1981). An Exponential Family of Probability Distributions
440 for Directed Graphs. *Journal of the American Statistical Association* 76, 33–65.
- 441 Ishiguro, K., Iwata, T., Ueda, N. & Tenenbaum, J. (2010). Dynamic infinite relational model
442 for time-varying relational data analysis. In *Advances in Neural Information Processing*
443 *Systems (NIPS)*.
- 444 Jamali-Rad, H., & Leus, G. (2012). Dynamic Multidimensional Scaling for Low-Complexity
445 Mobile Network Tracking. *IEEE Transactions on Signal Processing* 60, 4485–4491.

- 446 Kastner, G., Frühwirth-Schnatter, S., & Lopes, H.F. (2013) Analysis of Exchange Rates
 447 via Multivariate Bayesian Factor Stochastic Volatility Models. In Lanzarone E., &
 448 Ieva, F. *The Contribution of Young Researchers to Bayesian Statistics, Proceedings of*
 449 *BAYSM2013*. 63, Springer.
- 450 Kemp, C., Tenenbaum, J. B., Griffiths, T. L., Yamada, T. & Ueda, N. (2006). Learning
 451 systems of concepts with an infinite relational model. *In Proceedings of the 21st National*
 452 *Conference on Artificial Intelligence*.
- 453 Nakajima, J., & West, M. (2012) Dynamic factor volatility modeling: A Bayesian latent
 454 threshold approach. *Journal of Financial Econometrics* 11, 116–153.
- 455 Nowicki, K., & Snijders, T.A.B. (2001). Estimation and prediction for stochastic block-
 456 structures. *Journal of the American Statistical Association* 96, 1077–1087.
- 457 Oh, M.S., & Raftery A.E. (2007). Model-based clustering with dissimilarities: A Bayesian
 458 approach. *Journal of Computational and Graphical Statistics* 16, 559–585.
- 459 Oh, M.S., & Raftery A.E. (2001). Bayesian Multimensional scaling and choice of dimension.
 460 *Journal of the American Statistical Association* 96, 1031–1004.
- 461 Polson, N.G., Scott J.G., & Windle J. (2013). Bayesian inference for logistic models using
 462 Polya-Gamma latent variables. <http://arxiv.org/abs/1205.0310>.
- 463 Robins, G.L., & Pattison, P.E., (2001). Random graph models for temporal processes in
 464 social networks. *Journal of Mathematical Sociology* 25, 5–41.
- 465 Ross, S. (1976). The arbitrage theory of capital asset pricing. *Journal of Finance* 13,
 466 341–360.
- 467 Sarkar, P., Siddiqi, S.M., & Gordon, G.J. (2007). A latent space approach to dynamic
 468 embedding of co-occurrence data. *In Proceedings of the 11th International Conference on*
 469 *Artificial Intelligence and Statistics (AI-STATS)*.
- 470 Sarkar, P., & Moore, A.W. (2005). Dynamic social network analysis using latent space
 471 models. *In Advances in Neural Information Processing Systems (NIPS)*.
- 472 Sharpe, W. (1964). Capital asset prices: a theory of market equilibrium under conditions
 473 of risk. *Journal of Finance* 19, 425–442.
- 474 Snijders, T.A.B. (2002). Markov Chain Monte Carlo Estimation of Exponential Random
 475 Graph Models. *Journal of Social Structure* 2, 1–40.
- 476 Strauss, D., & Ikeda, M. (1990). Pseudolikelihood Estimation for Social Networks. *Journal*
 477 *of the American Statistical Association* 49, 204–212.
- 478 Tsay, R.S. (2005). *Analysis of Financial Time Series*. II ed., Wiley.
- 479 Wilson, A.G. & Ghahramani Z. (2010). Generalised Wishart Processes. <http://arxiv.org/abs/1101.0240>.

- 481 Xing, E.P., Fu, W., & Song, L. (2010). A State-Space Mixed Membership Blockmodel for
 482 Dynamic Network Tomography. *The Annals of Applied Statistics* 4, 535–566.
- 483 Xu, S.K., & Hero III, A.O., (2013). Dynamic stochastic blockmodels: Statistical models for
 484 time-evolving networks <http://arxiv.org/abs/1304.5974>.
- 485 Yang, T.B, Chi, Y., Zhu, S.H., Gong, Y.H., & Jin, R. (2011). Detecting communities and
 486 their evolutions in dynamic social networks—a Bayesian approach. *Machine Learning* 82,
 487 157–189.
- 488 Zhu, B., & Dunson, D.B. (2012). Locally Adaptive Bayes Nonparametric Regression via
 489 Nested Gaussian Processes. <http://arxiv.org/abs/1201.4403>.

490 **7. Appendix**

Proof of Theorem 3: Since \mathcal{T} is compact, for every $\epsilon_0 > 0$ there exists an open covering of ϵ_0 -balls $B_{\epsilon_0}(t_0) : \{t : \|t - t_0\|_2 < \epsilon_0\}$ with a finite subcover such that $\mathcal{T} \subset \cup_{t_0 \in \mathcal{T}_0} B_{\epsilon_0}(t_0)$, where $|\mathcal{T}_0| = T$. Then:

$$\Pi_S \left(\sup_{t \in \mathcal{T}} \|S(t) - S^*(t)\|_2 < \epsilon \right) = \Pi_S \left(\max_{t_0 \in \mathcal{T}_0} \sup_{t \in B_{\epsilon_0}(t_0)} \|S(t) - S^*(t)\|_2 < \epsilon \right).$$

Define $Z(t_0) = \sup_{t \in B_{\epsilon_0}(t_0)} \|S(t) - S^*(t)\|_2$. Since

$$\Pi_S \left(\max_{t_0 \in \mathcal{T}_0} Z(t_0) < \epsilon \right) > 0 \iff \Pi_S (Z(t_0) < \epsilon) > 0, \forall t_0 \in \mathcal{T}_0$$

491 we only need to look at each ϵ_0 -ball independently as follow:

$$\begin{aligned} & \Pi_S \left(\sup_{t \in B_{\epsilon_0}(t_0)} \|S(t) - S^*(t)\|_2 < \epsilon \right) \\ & \geq \Pi_S \left(\|S(t_0) - S^*(t_0)\|_2 + \sup_{t \in B_{\epsilon_0}(t_0)} \|S^*(t_0) - S^*(t)\|_2 + \sup_{t \in B_{\epsilon_0}(t_0)} \|S(t_0) - S(t)\|_2 < \epsilon \right) \\ & \geq \Pi_S \left(\|S(t_0) - S^*(t_0)\|_2 < \frac{\epsilon}{3} \right) \Pi_S \left(\sup_{t \in B_{\epsilon_0}(t_0)} \|S^*(t_0) - S^*(t)\|_2 < \frac{\epsilon}{3} \right) \Pi_S \left(\sup_{t \in B_{\epsilon_0}(t_0)} \|S(t_0) - S(t)\|_2 < \frac{\epsilon}{3} \right) \end{aligned} \tag{6}$$

492 Where the first inequality comes from repeated uses of triangle inequality, and the second
 493 follows from the fact that each of these terms is an independent event. We evaluate each of
 494 these terms in turn.

Based on the continuity of $S^*(\cdot)$, for all $\epsilon/3 > 0$, there exists an $\epsilon_{0,1} > 0$ such that:

$$\|S(t_0) - S^*(t_0)\|_2 < \frac{\epsilon}{3}, \quad \forall \|t - t_0\|_2 < \epsilon_{0,1}$$

495 Therefore, $\Pi_S \left(\sup_{t \in B_{\epsilon_{0,1}}(t_0)} \|S^*(t_0) - S^*(t)\|_2 < \frac{\epsilon}{3} \right) = 1$.

Given the GP prior on the elements of $X(\cdot)$ and letting $x_{ih}(t) = [X(t)]_{ih}$, the equation

$$[X(t)X(t)']_{ij} = \sum_{h=1}^H x_{ih}(t)x_{jh}(t), \quad \forall t \in \mathcal{T}$$

represents a finite sum over pairwise products of almost surely continuous functions (recalling GP assumption on the elements x_{ih}) and thus result in a matrix $X(t)X(t)'$ with elements almost surely continuous on \mathcal{T} . Therefore $S(t) = \mu(t) \times 1_V 1'_V + X(t)X(t)'$ is almost surely continuous on \mathcal{T} since the baseline $\mu(\cdot)$ is itself almost surely continuous given the GP prior assumption. Therefore, similarly as before, for all $\epsilon/3 > 0$, there exists and $\epsilon_{0,2} > 0$ such that:

$$\Pi_S \left(\sup_{t \in B_{\epsilon_{0,2}}(t_0)} \|S(t_0) - S(t)\|_2 < \frac{\epsilon}{3} \right) = 1$$

To examine last term, first note that:

$$\Pi_S \left(\|S(t_0) - S^*(t_0)\|_2 < \frac{\epsilon}{3} \right) = \Pi_S \left(\|\mu(t_0) \times 1_V 1'_V + X(t_0)X(t_0)' - \mu^*(t_0) \times 1_V 1'_V - X(t_0)^* X(t_0)^{*'}\|_2 < \frac{\epsilon}{3} \right)$$

Where $\{X(t_0)^*, \mu^*(t_0)\}$ is any element of $\mathcal{X}_X \otimes \mathcal{X}_\mu$ such that $S^*(t_0) = \mu^*(t_0) \times 1_V 1'_V + X(t_0)^* X(t_0)^{*'}$. Such a factorization exists by Corollary 2. Thus, using triangle inequality, we can bound this probability by:

$$\begin{aligned} & \Pi_S \left(\|S(t_0) - S^*(t_0)\|_2 < \frac{\epsilon}{3} \right) \\ & \geq \Pi_S \left(\|X(t_0)X(t_0)' - X(t_0)^* X(t_0)^{*'}\|_2 < \frac{\epsilon}{6} \right) \Pi_\mu \left(\|1_V 1'_V (\mu(t_0) - \mu^*(t_0))\|_2 < \frac{\epsilon}{6} \right) \end{aligned}$$

Based on the support of the Gaussian prior,

$$\Pi_\mu \left(\|1_V 1'_V (\mu(t_0) - \mu^*(t_0))\|_2 < \frac{\epsilon}{6} \right) = \Pi_\mu \left(|(\mu(t_0) - \mu^*(t_0))| < \frac{\epsilon}{6\sqrt{V}} \right) > 0.$$

For studying the first term of the previous decomposition note that:

$$X(t_0)X(t_0)' \{ \tau_h \}_{h=1}^H = \sum_{h=1}^H x_h(t_0)x_h(t_0)'$$

where $x_h(t_0) = [x_{1h}(t_0), \dots, x_{Vh}(t_0)]'$ is distributed, according to our prior specification, as $N_V(0, \tau_h^{-1} I_V)$, implying that $x_h(t_0)x_h(t_0)' | \tau_h \sim W_V(1, \tau_h^{-1} I_V)$ independently for all $h = 1, \dots, H$, where $W_V(\cdot, \cdot)$ denotes the Wishart random variable. Using the triangle inequality we obtain:

$$\Pi_S \left(\|X(t_0)X(t_0)' - X(t_0)^* X(t_0)^{*'}\|_2 < \frac{\epsilon}{6} \right) \geq \prod_{h=1}^H \Pi_{x_h} \left(\|x_h(t_0)x_h(t_0)' - x_h(t_0)^* x_h(t_0)^{*'}\|_2 < \frac{\epsilon}{6H} \right)$$

Since $x_h(t_0)^* x_h(t_0)^{*'}$ is an arbitrary rank-1 symmetric matrix in $\Re^{V \times V}$, and based on the support of the Wishart distribution:

$$\Pi_{x_h} \left(\|x_h(t_0)x_h(t_0)' - x_h(t_0)^* x_h(t_0)^{*'}\|_2 < \frac{\epsilon}{6H} \right) > 0, \quad \forall h = 1, \dots, H.$$

Thus $\Pi_S \left(\|X(t_0)X(t_0)' - X(t_0)^* X(t_0)^{*'}\|_2 < \frac{\epsilon}{6} \right) > 0$ and combining it with the large support property previously proved for the prior on the baseline $\mu(\cdot)$, we have:

$$\Pi_S \left(\|S(t_0) - S^*(t_0)\|_2 < \frac{\epsilon}{3} \right) > 0$$

For every $S^*(\cdot)$ and $\epsilon > 0$, let $\epsilon_0 = \min(\epsilon_{0,1}, \epsilon_{0,2})$, with $\epsilon_{0,1}$ and $\epsilon_{0,2}$ defined as above. Then, combining the positivity results of each of the three terms in 6 completes the proof.